nanocrystal synthesis and ligand exchange under support by U.S. Department of Energy, Office of Basic Energy Sciences, Division of Materials Sciences and Engineering under Award DE-SC0010334. D.F.H., A.R., N.K., S.K., L.C.S., and J.W.P. were supported for nitrogenase purification and product quantification as part of the Biological and Electron Transfer and Catalysis (BETCy) EFRC, an Energy Frontier Research Center funded by the U.S. Department of Energy, Office of Science (DE-SC0012518). The authors thank W. Tumas and R. Greene for thoughtful advice and many helpful discussions, and B. Hoffman for helpful discussions and constructive reading of the manuscript. Data are available in the supplementary materials. K.A.B. preformed photochemical experiments, including colorimetric NH_3 measurements; N.K., A.R., D.F.H., and S.K. preformed nitrogenase and MoFe protein purifications, physiological nitrogenase assays, and fluorometric NH_3 measurements; M.B.W. and H.H. performed CdS nanocrystal synthesis, ligand exchange, and transmission electron microscopy imaging; K.A.B, L.C.S., G.D., J.W.P., and P.W.K. conceived and designed the study. All authors contributed to the writing of the manuscript.

SUPPLEMENTARY MATERIALS

www.sciencemag.org/content/352/6284/448/suppl/DC1
Materials and Methods
Figs. S1 to S3
Tables S1 to S13
References (*23*–*28*)

15 January 2016; accepted 23 March 2016
10.1126/science.aaf2091

PALEONTOLOGY

Precocity in a tiny titanosaur from the Cretaceous of Madagascar

Kristina Curry Rogers,[1]* Megan Whitney,[2] Michael D'Emic,[3] Brian Bagley[4]

Sauropod dinosaurs exhibit the largest ontogenetic size range among terrestrial vertebrates, but a dearth of very young individuals has hindered understanding of the beginning of their growth trajectory. A new specimen of *Rapetosaurus krausei* sheds light on early life in the smallest stage of one of the largest dinosaurs. Bones record rapid growth rates and hatching lines, indicating that this individual weighed ~3.4 kilograms at hatching. Just several weeks later, when it likely succumbed to starvation in a drought-stressed ecosystem, it had reached a mass of ~40 kilograms and was ~35 centimeters tall at the hip. Unexpectedly, *Rapetosaurus* limb bones grew isometrically throughout their development. Cortical remodeling, limb isometry, and thin calcified hypertrophic metaphyseal cartilages indicate an active, precocial growth strategy.

Sauropod dinosaurs began life as hatchlings less than a meter long and 10 kg in body mass (*1*). From there, they grew to immense adult body sizes, achieving the greatest absolute ontogenetic size difference known for any terrestrial tetrapod group. Sauropod eggs containing embryos dispelled the misconception that sauropods were viviparous (*1*), but lack of data at critical perinatal ontogenetic intervals has hindered our understanding of the beginning of sauropod life history. Here we describe a diminutive *Rapetosaurus krausei* (Université d'Antananarivo UA 9998) collected from a single bone-bearing horizon at locality MAD 93-18 in the Upper Cretaceous Anembalemba Member of the Maevarano Formation (*2*, *3*) (fig. S1). UA 9998 includes limb, girdle, and vertebral elements indistinguishable from those of other, larger *Rapetosaurus* specimens (*3*–*5*) (Fig. 1, figs. S2 and S3, and tables S1 and S2). The lengths of preserved hind limb elements suggest a hip height of ~35 cm, and autopodial scaling and developmental mass extrapolation (*6*) yield an estimated body mass of ~40 kg (*3*) (Fig. 1 and tables S2 and S3). We use bone histology and x-ray computed tomography (XRCT) (*3*) (table S4) to understand growth dynamics in perinatal *Rapetosaurus*.

[1]Biology and Geology Departments, Macalester College, St. Paul, MN 55105, USA. [2]Department of Biology, University of Washington, Seattle, WA 98185-1800, USA. [3]Biology Department, Adelphi University, Garden City, NY 11530-0701, USA. [4]Department of Earth Sciences, University of Minnesota, Minneapolis, MN 55455-1333, USA.
*Corresponding author. Email: rogersk@macalester.edu

Long bone cortices are almost exclusively composed of densely vascularized fibrolamellar primary bone tissue. Osteocyte lacunae are densely distributed within the woven bone component of the fibrolamellar complex (Fig. 2), and centripetal bone deposition within primary vascular canals diminishes porosity in deeper cortex regions. External, subperiosteal vascular canals retain an enlarged diameter because osteonal infilling had only just begun. Most primary vascular canals are longitudinal, but XRCT data highlight abundant anastomosing circular and radial canals (Fig. 3, MorphoBank, Project 2326). Lines of arrested growth (LAG) and annuli are absent in all elements, but a nearly ubiquitous perimedullar modulation of vascularity is represented by a ~435-μm-wide circumferential zone (Figs. 2, A to C, and 3) that is the consequence of one or two consecutive layers of primary vascular canals with diameters ~20 μm narrower than canals positioned in the deeper or more superficial cortex (Fig. 2, B and C). Zone morphology is consistent with hatching lines observed in squamates (*7*) and crocodilians (*8*), neonatal lines observed in mammals (*9*), and neonatal vascular transitions recorded in some mammals (*10*) and birds (*11*) (fig. S4). Hatching lines archive perinatal limb bone circumferences for UA 9998, and an isometric model of limb growth predicts a hind limb length of ~20 cm and a body mass of 2.5 to 4.3 kg at hatching (*3*) (tables S3 and S5). These data align with hypothesized sauropod hatchling sizes based on known egg dimensions and embryonic remains [e.g., (*1*)]. Daily appositional rates for fibrolamellar bone tissue in three nonavian dinosaurs that bracket *Rapetosaurus* phylogenetically (*12*) suggest that 39 to 77 days transpired between hatching and the death of UA 9998.

A single generation of scattered secondary osteons exists in the midcortex of all elements (Figs. 2, A, B, and D, and 3). Proximal and distal ends of long bones preserve the calcified hypertrophic cartilage (CHC) component of the metaphyses and epiphyses (Figs. 1D and 4). The CHC regions are ~500 μm thick, with thicknesses varying slightly among elements and between proximal and distal ends of a single bone: In the tibia, the CHC is thicker at the proximal end (Fig. 4, A to C). The chondrocytes that form the CHC are spherical and exhibit a columnar orientation, particularly at the metaphyses (Fig. 4, D and E). The deep surface of the metaphysis is sharply demarcated and linear where endosteal bone has replaced calcified cartilage (Fig. 4D). Some metaphyseal vessels invade the zone of hypertrophy, and bone infiltrates the epiphyseal region at the margins of canals to result in small islands of hypertrophied chondrocytes within bony trabeculae more than a millimeter deep to the proximal and distal surfaces of the tibia (Fig. 4E).

Despite massive changes in body size throughout ontogeny, general morphology and proportions among appendicular elements of UA 9998 indicate that *Rapetosaurus* limb bones are similar in shape throughout life (*3*) (fig. S3 and table S2). Selection may act strongly on juvenile morphologies in precocial species and can lead to "ontogenetic canalization," resulting in close resemblance of adults and juveniles [e.g., (*13*, *14*)]. Lack of noticeable allometry in the long bones of neosauropods highlights the efficiency of long-limbed locomotion in adults (*15*) and might also indicate that early in ontogeny, locomotor scope was more varied than in adults, with a wider gait repertoire possible in young "overbuilt" juveniles [e.g., (*15*, *16*)]. Similar patterns are documented for some mammals, in which the shape and relative proportions of skeletal elements scale isometrically to maintain mechanical integrity during rapid growth (*16*, *17*). Maintenance of isometric relationships through ontogeny has recently been ascribed to a complex mechanism of bone scaling based on element-specific balance between proximal and distal epiphyseal growth rates combined with synchronous and directed bone remodeling (*17*). The single generation of secondary osteons extending into the midcortex of all sampled perinatal *Rapetosaurus* elements (Figs. 2D and 3)

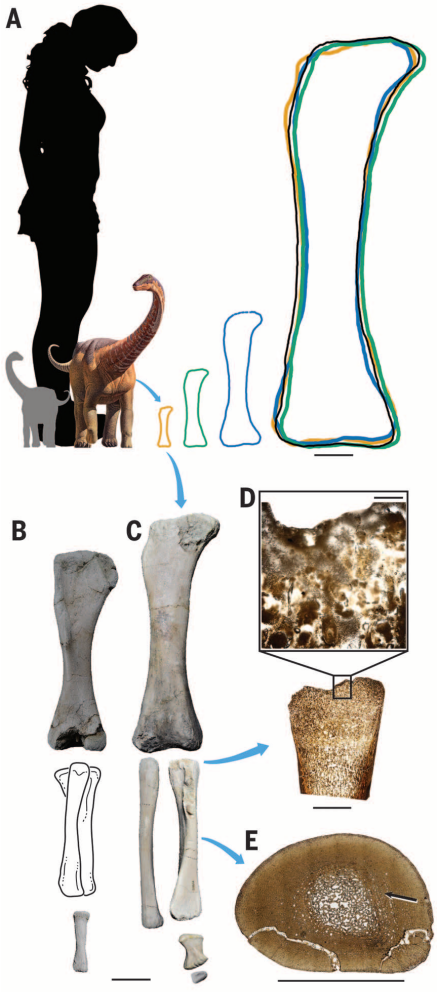

Fig. 1. Perinate *Rapetosaurus krausei* (UA 9998). (**A**) Isometric growth of limb elements illustrated by four femora throughout ontogeny. Gray silhouette represents hatchling, color represents UA 9998. Orange outline is UA 9998, black is largest known *Rapetosaurus* (length = 143 cm), green and blue are intermediate *Rapetosaurus* femora (*3*–*5*) (figs. S2 and S3 and tables S1 to S3). (**B**) Right humerus, metacarpal III. (**C**) Right femur, fibula, metatarsal I, phalanx I.1, left tibia (reversed) in anterior view. High-resolution images archived at MorphoBank (Project 2326). (**D**) Proximal tibia epiphyseal microstructure. (**E**) Mid-diaphyseal tibia microstructure; arrow indicates hatching line. Scale bars: 20 cm (A), 3 cm (B and C), 500 μm [(D), inset], and 1 mm (D and E).

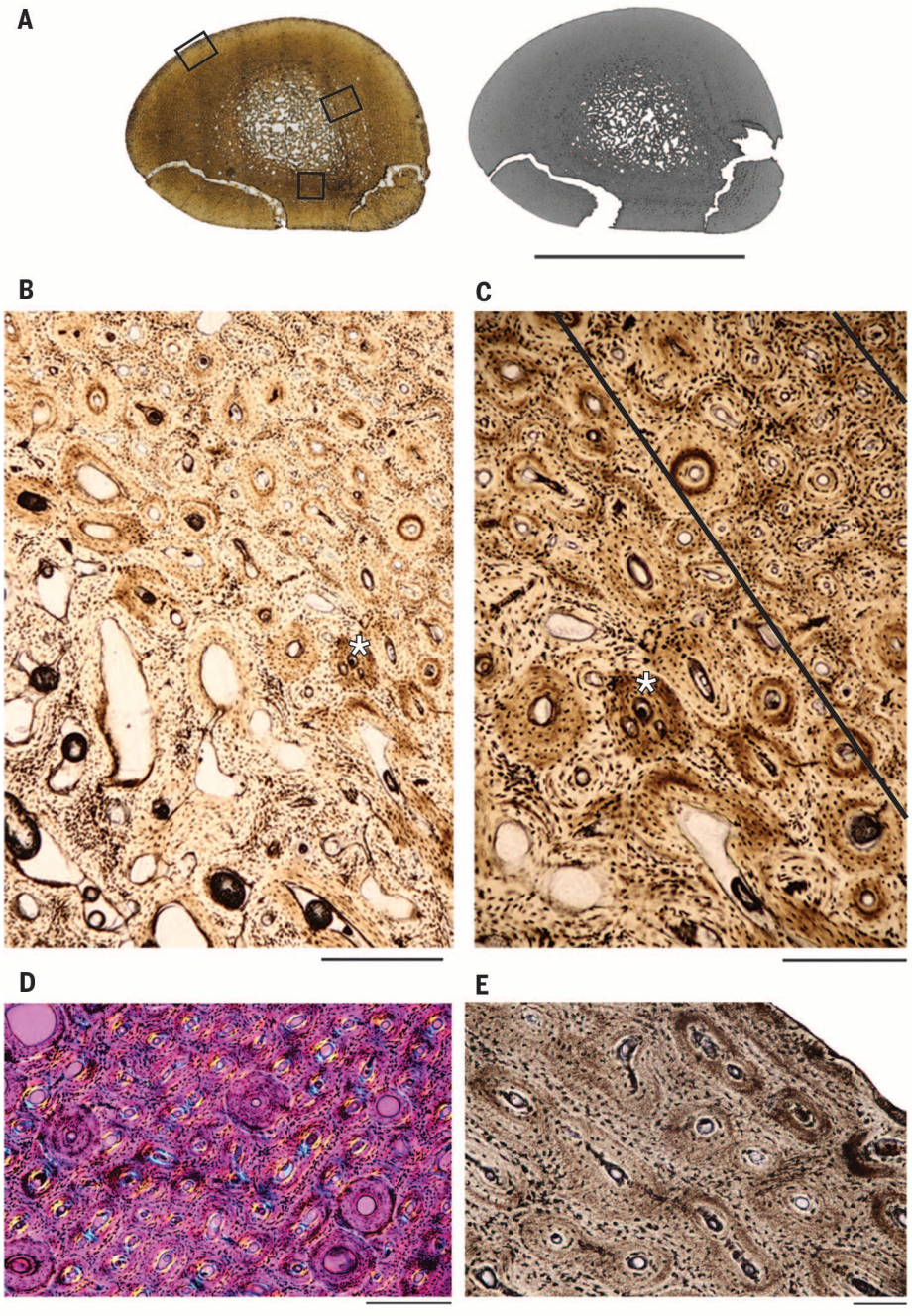

Fig. 2. Tibia mid-diaphyseal histology. (**A**) Histologic (left) and XRCT sections (right). Boxed areas are enlarged in (B) to (E). (**B**) Transition between embryonic (bottom left) and postnatal bone tissue (upper right); asterisk indicates the same location in (B) and (C). (**C**) Black bars bound hatching line zone, with decreased vascular canal dimensions. (**D**) Midcortex secondary remodeling in cross-polarized light. (**E**) Periosteal primary fibrolamellar bone. Scale bars: 1 cm (A), 500 μm (B), 300 μm (C and D), and 100 μm (E).

contrasts with other known dinosaurs that exhibit midcortex remodeling in "late juvenile" stages at the earliest (*18*, *19*). Additional explanations for the triggering of bone remodeling relate to a combination of factors, including (i) a high basal metabolic rate (*20*); (ii) biomechanical loading (*21*); (iii) aging and microfracture repair (*22*); and (iv) mineral storage and remobilization (*21*). Our data corroborate the idea that the postcranial skeletons of very young *Rapetosaurus* were built to accommodate the massive adult sizes that they would eventually achieve. Moreover, the early onset of bone remodeling in weight-bearing elements, combined with the isometry of the *Rapetosaurus* limb skeleton throughout ontogeny, bolsters an interpretation of precocity in this taxon.

The calcified cartilage components of the epiphyseal-metaphyseal region can help to differentiate fossil vertebrates along the altricial-precocial growth strategy spectrum [e.g., (*19*, *23*–*25*)]. In birds, longitudinal bone growth rates are higher and calcified cartilage metaphyseal structures are thicker in altricial hatchlings (*24*, *25*). In precocial birds, the reduced cartilage and increased bone content relate to balancing bone elongation and functional constraints, particularly in fast-growing organisms (*24*, *25*), and calcified cartilage thickness declines posteclosion in accordance

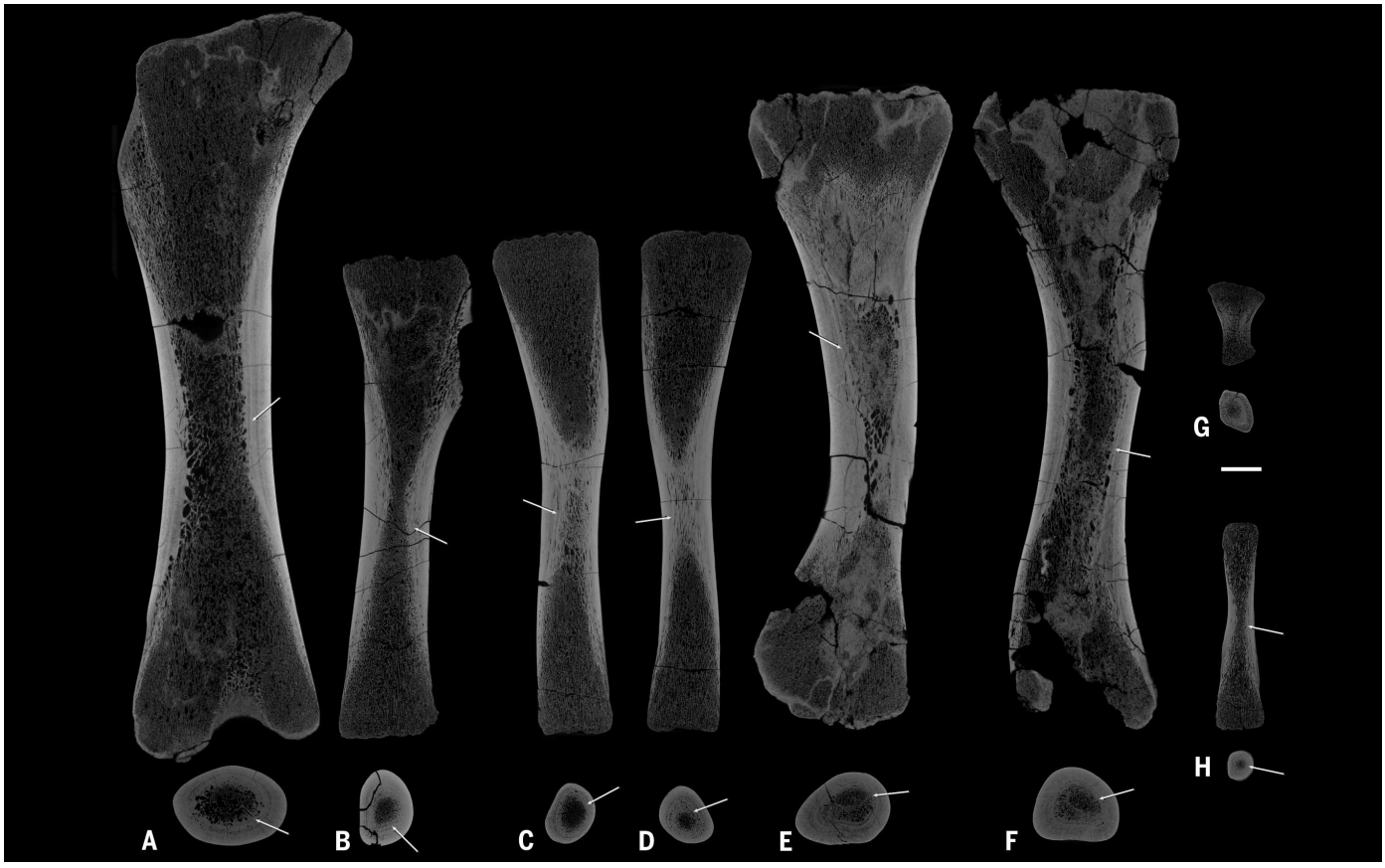

Fig. 3. Longitudinal and transverse XRCT sections. (**A**) Right femur; (**B**) left tibia; (**C**) right fibula; (**D**) left fibula; (**E**) right humerus; (**F**) left humerus; (**G**) right metatarsal I; (**H**) right metacarpal III. Arrows indicate hatching line. Scale bar: 1 cm.

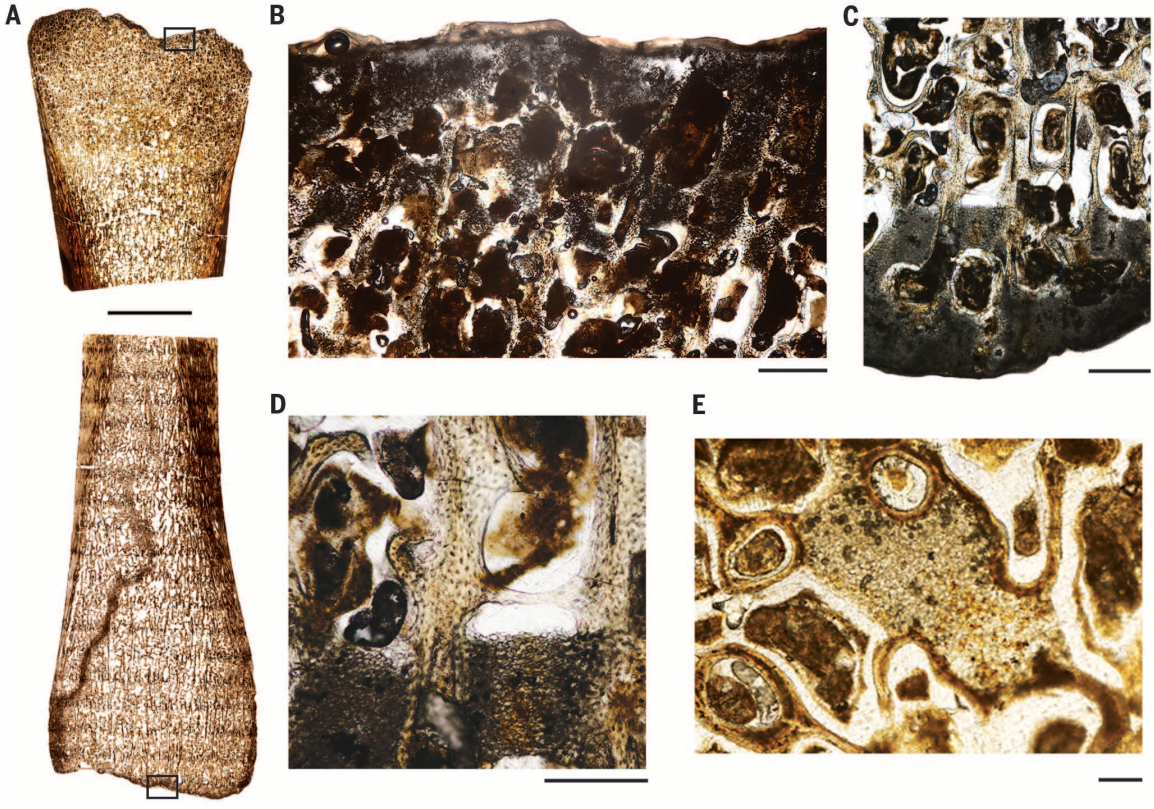

Fig. 4. Tibia epiphyseal histology. (**A**) Proximal (top) and distal sections (bottom). Boxed areas are enlarged in (B) and (C). (**B**) Proximal calcified hypertrophic cartilage (CHC). (**C**) Distal CHC. (**D**) Metaphyseal region of the distal tibia illustrating stout, sharp metaphyseal CHC. (**E**) Proximal metaphysis preserves CHC "islands" within bony trabeculae. Scale bars: 1 cm (A), 500 μm (B and C), 300 μm (D), and 100 μm (E).

with growth slowdown prior to fledging (*25*). Among other embryonic and perinatal dinosaurs, the thickness of the CHC has been used as a proxy for altriciality or precocity. Hadrosaurs *Maiasaura* and *Hypacrosaurus* preserve "massive amounts" of calcified cartilage and numerous diaphyseal cartilage islands hypothesized to indicate altricial behaviors (*18*, *19*). Epiphyseal histology of the theropod *Troodon* records thinner CHC with only a few small, deeply located cartilage islands within the diaphysis, consistent with a more precocial growth strategy (*19*), but, unlike titanosaurs, paravians (including *Troodon*) are thought to have some degree of parental care (*3*, *26*). UA 9998 CHC regions are thin (~500 μm), with sparse, deep cartilage islands that compare favorably with the CHC of precocial birds nearing fledging (*23*–*25*) and some perinatal dinosaurs (*19*). That said, UA 9998 is only ~11% the size of the largest known *Rapetosaurus* individual (*3*) (table S2), and it is unreasonable to assume that the thin CHC zones indicate growth slowdown at skeletal maturity. In extant vertebrates, bone elongation also slows during intervals of acute starvation via a decrease in chondroplasia and osteoblastic activity (*27*, *28*). These shifts in cellular activity are signaled by modified metaphyseal morphology as osteogenesis outpaces the rate of cartilage proliferation, eventually restricting the CHC to result in a "stouter" metaphysis with a "sharper" chondro-osseus junction than that in healthy individuals (*27*). UA 9998 exhibits the stout, sharp CHC expected with acute starvation (*27*, *28*). Drought and its attendant hardships have been well documented for the Maevarano Formation vertebrate assemblage [e.g., (*2*, *3*, *29*, *30*)]. During the short interval between hatching and drought-related mortality, UA 9998 lived an active, precocial life evidenced by isometric scaling, rapid neonatal growth rates, midcortical remodeling, and calcified cartilaginous metaphyseal morphology.

REFERENCES AND NOTES

1. L. M. Chiappe *et al.*, *Nature* **396**, 258–261 (1998).
2. R. R. Rogers, *Geology* **33**, 297–300 (2005).
3. Materials and methods are available as supplementary materials on *Science* Online.
4. K. Curry Rogers, C. A. Forster, *Nature* **412**, 530–534 (2001).
5. K. Curry Rogers, *J. Vertebr. Paleontol.* **29**, 1046–1086 (2009).
6. G. M. Erickson, T. A. Tumanova, *Zool. J. Linn. Soc.* **130**, 551–566 (2000).
7. J. Hugi, M. R. Sánchez-Villagra, *J. Herpetol.* **46**, 312–324 (2012).
8. J. Castanet, H. Francillon-Viellot, F. J. Meunier, A. de Ricqlès, in *Bone*, vol. 7, *Bone Growth—B*, B. K. Hall, Ed. (CRC Press, 1993), chap. 9.
9. J. Castanet *et al.*, *J. Zool.* **263**, 31–39 (2004).
10. A. J. Curtin, A. A. Macdowell, E. G. Schaible, V. Louise Roth, *J. Vertebr. Paleontol.* **32**, 939–955 (2012).
11. J. M. Starck, A. Chinsamy, *J. Morphol.* **254**, 232–246 (2002).
12. J. Cubo, N. Le Roy, C. Martinez-Maza, L. Montes, *Paleobiology* **38**, 335–349 (2012).
13. D. R. Carrier, *Physiol. Zool.* **69**, 467–488 (1996).
14. D. R. Carrier, R. Leon, *J. Zool. (Lond.)* **222**, 375–389 (1990).
15. M. F. Bonnan, *Anat. Rec.* **290**, 1089–1111 (2007).
16. A. A. Biewener, *J. Exp. Biol.* **208**, 1665–1676 (2005).
17. T. Stern *et al.*, *PLOS Biol.* **13**, e1002212 (2015).
18. J. R. Horner, A. de Ricqlès, K. Padian, *J. Vertebr. Paleontol.* **20**, 115–129 (2000).
19. J. R. Horner, K. Padian, A. de Ricqlès, *Paleobiology* **27**, 39–58 (2001).
20. A. Teti, A. Zallone, *Bone* **44**, 11–16 (2009).
21. A. G. Robling, A. B. Castillo, C. H. Turner, *Annu. Rev. Biomed. Eng.* **8**, 455–498 (2006).
22. R. B. Martin, *Calcif. Tissue Int.* **73**, 101–107 (2003).
23. C. Barreto, R. M. Albrecht, D. E. Bjorling, J. R. Horner, N. J. Wilsman, *Science* **262**, 2020–2023 (1993).
24. J. M. Starck, R. E. Ricklefs, *Avian Growth and Development: Evolution Within the Altricial-Precocial Spectrum* (Oxford Univ. Press, 1998).
25. L. Montes, E. de Margerie, J. Castanet, A. de Ricqlès, J. Cubo, *J. Anat.* **206**, 445–452 (2005).
26. D. J. Varricchio *et al.*, *Science* **322**, 1826–1828 (2008).
27. R. M. Acheson, M. N. Macintyre, *Br. J. Exp. Pathol.* **39**, 37–45 (1958).
28. R. M. Acheson, *J. Anat.* **93**, 123–130 (1959).
29. R. R. Rogers, D. W. Krause, K. Curry Rogers, *Nature* **422**, 515–518 (2003).
30. R. R. Rogers, D. W. Krause, K. Curry Rogers, A. Rasoamiaramanana, L. Rahantarisoa, *J. Vertebr. Paleontol.* **27** (suppl. 2), 21–31 (2007).

ACKNOWLEDGMENTS

Research was supported by the National Science Foundation (EAR-0955716). Higher-resolution images and XRCT .mpg files are archived at MorphoBank (http://morphobank.org/permalink/?P2326). Original fossil material will be permanently reposited in the paleontology collection at the Université d'Antananarivo, with exact replicas (casts) housed at the Denver Museum of Nature and Science and at Macalester College. We thank the people of Berivotra and the Mahajanga Basin Project. R. Rogers, P. O'Connor, and three reviewers provided insightful comments. We thank J. Groenke and V. Heisey for preparation, J. Thole for photos, and T. Keillor, R. Martin, and D. Vital for artwork.

SUPPLEMENTARY MATERIALS

www.sciencemag.org/content/352/6284/450/suppl/DC1
Materials and Methods
Supplementary Text
Figs. S1 to S4
Tables S1 to S5
References (*31*–*75*)

24 December 2015; accepted 25 March 2016
10.1126/science.aaf1509

CELL QUIESCENCE

RNA-binding proteins ZFP36L1 and ZFP36L2 promote cell quiescence

Alison Galloway,[1] Alexander Saveliev,[1] Sebastian Łukasiak,[1]* Daniel J. Hodson,[1,2] Daniel Bolland,[3] Kathryn Balmanno,[4] Helena Ahlfors,[1] Elisa Monzón-Casanova,[1,5] Sara Ciullini Mannurita,[1]† Lewis S. Bell,[1] Simon Andrews,[6] Manuel D. Díaz-Muñoz,[1] Simon J. Cook,[4] Anne Corcoran,[3] Martin Turner[1]‡

Progression through the stages of lymphocyte development requires coordination of the cell cycle. Such coordination ensures genomic integrity while cells somatically rearrange their antigen receptor genes [in a process called variable-diversity-joining (VDJ) recombination] and, upon successful rearrangement, expands the pools of progenitor lymphocytes. Here we show that in developing B lymphocytes, the RNA-binding proteins (RBPs) ZFP36L1 and ZFP36L2 are critical for maintaining quiescence before precursor B cell receptor (pre-BCR) expression and for reestablishing quiescence after pre-BCR–induced expansion. These RBPs suppress an evolutionarily conserved posttranscriptional regulon consisting of messenger RNAs whose protein products cooperatively promote transition into the S phase of the cell cycle. This mechanism promotes VDJ recombination and effective selection of cells expressing immunoglobulin-μ at the pre-BCR checkpoint.

Lymphocyte development is characterized by dynamic shifts between quiescence and proliferation. Quiescence promotes variable-diversity-joining (VDJ) recombination, the process that generates immunoglobulin and T cell receptor genes, because RAG2 protein expression is restricted to the G_0-G_1 phase of the cell cycle (*1*–*3*). In B cells, VDJ recombination leads to expression of an immunoglobulin-μ (Igμ) heavy chain that, together with the surrogate light chains, forms a precursor B cell receptor (pre-BCR). Signals from the pre-BCR terminate the recombination process and trigger rapid proliferation associated with passage through the pre-BCR checkpoint (*4*). Later signals from the pre-BCR reestablish quiescence, allowing immunoglobulin light-chain recombination (fig. S1A) (*5*, *6*).

The ZFP36 family of RNA-binding proteins (RBPs) regulate gene expression posttranscriptionally by promoting mRNA decay (*7*). This requires their direct binding to AU-rich elements (AREs) located in the 3′ untranslated regions (3'UTRs) of mRNAs. ZFP36 destabilizes cytokine mRNAs and exerts an anti-inflammatory function (*8*, *9*). In addition, ZFP36 antagonizes *Myc*-induced lymphomagenesis (*10*), and its paralogs ZFP36L1 and ZFP36L2 have redundant roles in preventing T cell leukemia in mice (*11*). The pathways controlled by these RBPs, however, have remained poorly understood.

[1]Laboratory of Lymphocyte Signalling and Development, The Babraham Institute, Cambridge CB22 3AT, UK. [2]Department of Haematology, University of Cambridge, The Clifford Allbutt Building, Cambridge Biomedical Campus, Hills Road, Cambridge CB2 0AH, UK. [3]Laboratory of Nuclear Dynamics, The Babraham Institute, Cambridge CB22 3AT, UK. [4]Laboratory of Signalling, The Babraham Institute, Cambridge CB22 3AT, UK. [5]Department of Biochemistry, University of Cambridge, Tennis Court Road, Cambridge CB2 1QW, UK. [6]Bioinformatics Group, The Babraham Institute, Cambridge CB22 3AT, UK.
*Present address: Wellcome Trust Sanger Institute, Hinxton, Cambridge CB10 1SA, UK. †Present address: Department of Neuroscience, Psychology, Pharmacology and Child Health (NEUROFARBA), Child Health Section, University of Florence, Meyer Children's Hospital, Florence, Italy. **‡Corresponding author. Email: martin.turner@babraham.ac.uk**

Precocity in a tiny titanosaur from the Cretaceous of Madagascar

Kristina Curry Rogers, Megan Whitney, Michael D'Emic and Brian Bagley

Science **352** (6284), 450-453.
DOI: 10.1126/science.aaf1509

Tiny giant

Titanosaurs were the largest land vertebrates to have evolved, but even they had to start small. Curry Rogers *et al.* describe a baby *Rapetosaurus* only 35 cm at the hip at death. Histological and limb analysis suggest that this tiny giant had a much greater range of movement than it would have had as an adult. Furthermore, the work confirms hypotheses that these largest of dinosaurs were precocial, being able to move independently immediately after birth. This pattern differs from that seen in many contemporary dinosaur groups, such as theropods and ornithischians, for which increasing evidence suggests that parental care was important.

Science, this issue p. 450